Elliptic flow of thermal photons in Au+Au collisions at $\sqrt{s_{NN}} = 200$ GeV

Fu-Ming Liu,[1] Tetsufumi Hirano,[2] Klaus Werner,[3] and Yan Zhu[1]

[1] *Institute of Particle Physics, Central China Normal University, Wuhan, China*
[2] *Department of Physics, The University of Tokyo, 113-0033, Japan*
[3] *Laboratoire SUBATECH, University of Nantes - IN2P3/CNRS - Ecole desMines, Nantes, France*

(Dated: August 17, 2009)

The transverse momentum ($p_{\rm t}$) dependence, the centrality dependence and the rapidity dependence of the elliptic flow of thermal photons in Au+Au collisions at $\sqrt{s_{NN}} = 200$ GeV are predicted, based on a three-dimensional ideal hydrodynamic description of the hot and dense matter. The elliptic flow parameter v_2, i.e. the second Fourier coefficient of azimuthal distribution, of thermal photons, first increases with $p_{\rm t}$ and then decreases for $p_{\rm t} > 2$ GeV/c, due to the weak transverse flow at the early stage. The $p_{\rm t}$-integrated v_2 first increases with centrality, reaches a maximum at about 50% centrality, and decreases. The rapidity dependence of the elliptic flow $v_2(y)$ of direct photons (mainly thermal photons) is very sensitive to the initial energy density distribution along longitudinal direction, which provides a useful tool to extract the realistic initial condition from measurements.

PACS numbers:

I. INTRODUCTION

The deconfined and novel nuclear matter, the quark gluon plasma (QGP), has been expected to appear in relativistic heavy ion collisions. Various signatures have been proposed to verify its existence [1]. Many experiments have been done so far to explore properties of the QGP at the Relativistic Heavy Ion Collider (RHIC) and will be done at the Large Hadron Collider (LHC). Experimental results indicate that the QGP is created at RHIC [2].

Collective flow, in particular elliptic flow, is an effective probe to investigate bulk properties of the QGP in nucleus-nucleus collisions at relativistic energies. In non-central collisions the overlapping reaction zone of two colliding nuclei has an anisotropic shape, like an almond, in the transverse plane. This leads to a preferred flow direction parallel to the impact parameter, and therefore the initial spatial anisotropy is carried over to momentum-space anisotropy [3]. The QGP created at the early stage expands, cools down, and finally forms a hadronic gas (HG) phase. Then hadrons still have strong rescatterings until freeze-out. So those hadrons do carry information on the asymmetric flow, but only concerning the freeze out surface.

Fortunately, in high energy heavy ion collisions, thermal photons can be produced during the whole history of the evolution of the hot and dense matter. Moreover the mean free path of photons is much larger than the transverse size of the bulk matter. So thermal photons produced in the interior of the plasma pass through the surrounding matter without any interaction. As a result, thermal photons provide information on flow asymmetries even from inside the bulk volume, not just its surface.

In this paper, we investigate the relation between the observables of thermal photons and the space-time evolution of the hot and dense matter for exploring QGP properties, based on a fully three dimensional (3D) ideal hydrodynamic description of expansion of the matter. Toward establishment of the relation, we calculate the second Fourier coefficient of azimuthal momentum distribution, the so-called elliptic flow coefficient v_2, for thermal photons in Au+Au collisions at $\sqrt{s_{NN}} = 200$ GeV at various centralities (0-70%).

In Sec. 2 we will briefly review the space-time evolution of the hot and dense matter using the 3D ideal hydrodynamics and the basic formula for the production of thermal photons. In Sec. 3, we will show our results on v_2 of thermal photons in Au+Au collisions at $\sqrt{s_{NN}} = 200$ GeV, its transverse momentum, centrality dependences and rapidity dependence. Section 4 is devoted to discussion and summary of our results.

II. BULK EVOLUTION, THERMAL PHOTONS, AND ELLIPTIC FLOW

In our calculation, a full 3D ideal hydrodynamic calculation [4, 5] is employed to describe the space-time evolution of the hot and dense matter created in Au+Au collisions at RHIC. The local thermal equilibrium is assumed to be reached at the initial time $\tau_0 = 0.6$ fm/c. The transverse flow is assumed to be zero at τ_0. We consider two scenarios to obtain entropy density (or energy density) at τ_0: one is a parameterization based on Glauber model[4, 5], and the other is based on flux tubes (string picture) realized in the EPOS model[6]. For these two initial conditions, we take the same hydrodynamic equations and equations of state. The initial energy density from the two scenarios has been plotted as a function space-time rapidity η_s in Fig.1, where the dashed lines refer to the parameterized initial conditions, and dotted lines to the EPOS case. One can see that the energy density decreases very rapidly with η_s in EPOS, while it has a plateau for $|\eta_s| < 2.5$ using parameterized ini-

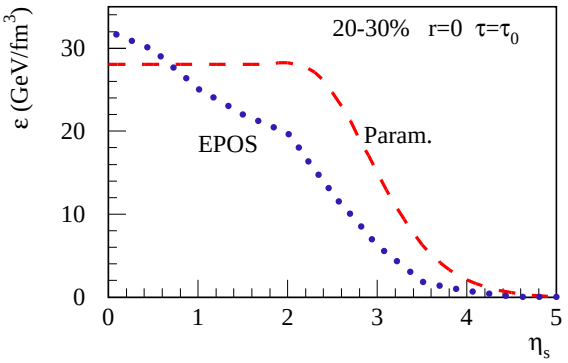

Figure 1: (Color online) energy density as a function of space-time η_s;Dashed lines from parameterized initial condition and dotted lines from EPOS initial condition.

tial conditions. In two dimensional hydrodynamics this plateau is assumed for the whole η_s region. The EPOS initial condition gives many similar results compared to the parameterized ones, *i.e.*, the measured $p_{\rm t}$-spectra of direct photons can also be well reproduced, and the same $p_{\rm t}$-dependence and centrality dependence of elliptic flow of thermal photons has been observed. But there are also striking differences, to be discussed later.

For both scenarios, the impact parameters corresponding to different centralities in Au+Au collisions at RHIC are 3.2, 5.5, 7.2, 8.5, 9.7, 10.8, and 11.7 fm for 0-10%, 10-20%, $\cdots$ and 60-70% centrality, respectively. The evolution of the fluid is governed by conservation laws of energy and momentum

$$\partial_\mu T^{\mu\nu} = 0 \tag{1}$$

with the energy-momentum tensor

$$T^{\mu\nu} = (e+P)u^\mu u^\nu - Pg^{\mu\nu} \tag{2}$$

for a perfect fluid. Here, e, P, and u^μ are energy density, pressure, and local four fluid velocity, respectively, which are related through the equation of state (EOS). The above equations are solved in full 3D space (τ, x, y, η_s) where τ, η_s, x, and y are the proper time, space-time rapidity, the two transverse coordinates along the impact parameter and perpendicular to the reaction plane, respectively. Since the net-baryon density is small near the mid-rapidity at RHIC, it is neglected. We also neglect the dissipative effects in the space-time evolution. The critical temperature of a first order phase transition between the QGP phase and the hadron phase is fixed at $T_c = 170$ MeV. The EOS for the QGP phase is

$$P = \frac{1}{3}(e - 4B), \tag{3}$$

where the bag constant is tuned to $B^{\frac{1}{4}} = 247.19$ MeV so that pressure of the QGP phase with three flavors is matched to that of HG phase (up to mass of $\Delta(1232)$) at T_c. In the hadronic phase, we employ two resonance gas models: partial chemical equilibrium (PCE) and full chemical equilibrium (FCE) [5]. In the PCE model, the particle ratios including contribution from resonance decays are assumed to keep during the hadronic expansion, which is required from the data of particle ratios. The PCE model is our standard choice to calculate the photon spectra in the following. For the purpose of comparison, we also employ the conventional resonance gas model in which chemical equilibrium is maintained during the hadronic expansion. In both models, the hadronic matter is kinetically and thermally frozen at $e^{\rm th} = 0.08$ GeV/fm^3. Corresponding freezeout temperature is $T^{\rm th} \sim 100$ (130) MeV for the PCE (FCE) model, which is consistent with the $p_{\rm t}$ slope of protons.

Transverse momentum spectra of thermal photons can be written as

$$\frac{dN}{dy\,d^2p_t} = \int d^4x\,\Gamma(E^*,T) \tag{4}$$

with $\Gamma(E^*,T)$ being the Lorentz invariant thermal photons emission rate which covers the contributions from the QGP phase [7] and HG phase [8], $d^4x = \tau\,d\tau\,dx\,dy\,d\eta_s$ being the volume-element, and $E^* = p^\mu u_\mu$ the photon energy in the local rest frame. Here p^μ is the photon's four momentum in the laboratory frame, T and u^μ are the temperature and the local fluid velocity, respectively, to be taken from the hydrodynamic calculations mentioned above. We only consider thermal photon radiation from the region with energy density above $e^{\rm th}$. For more details one can check [9] where the measured p_t spectra of direct photons at different centralities in Au+Au collisions are nicely reproduced.

The triple differential spectrum can be written as a Fourier series,

$$\frac{d^3N}{dy\,d^2p_t} = \frac{d^2N}{2\pi p_t\,dp_t\,dy}\left(1 + \sum_{n=1}^{\infty} 2v_n\cos(n\phi)\right), \tag{5}$$

where ϕ is the azimuthal angle of photon's momentum with respect to the reaction plane, which is defined to be the plane containing the impact parameter and beam axis. The elliptic flow is quantified by the second harmonic coefficient v_2

$$v_2(p_{\rm t},y) = \frac{\int d\phi\cos(2\phi)d^3N/dy\,d^2p_t}{\int d\phi d^3N/dy\,d^2p_t}. \tag{6}$$

The p_t dependence of the triple differential spectra is strongly affected by the flow u through the argument $E^* = p^\mu u_\mu$ in the photon emission rate. In the local rest frame thermal photons of any given energy are emitted isotropically. The isotropic distribution is Lorentz-boosted by flow velocity $\vec{v}_r$. The azimuthal asymmetry of the transverse components of the flow obviously ends up with an anisotropic momentum distribution, which gives a finite v_2. Therefore both strength and the anisotropy of transverse flow velocity are important to generate the

elliptic flow of thermal photons. To understand the thermal photon v_2 quantitatively, we define the mean radial flow $\langle v_r \rangle$ and the mean anisotropy of flow $\left\langle v_2^{\rm hydro} \right\rangle$ as

$$\langle v_r \rangle = \left\langle \sqrt{v_x^2 + v_y^2} \right\rangle \quad (7)$$

$$\left\langle v_2^{\rm hydro} \right\rangle = \langle \cos 2\phi_v \rangle = \left\langle \frac{v_x^2 - v_y^2}{v_x^2 + v_y^2} \right\rangle, \quad (8)$$

where $\langle \cdots \rangle$ stands for energy-density-weighted space-time average, v_x and v_y are the flow velocity components along x-axis and y-axis, respectively. We only consider the region above $e = e^{\rm th} = 0.08$ GeV/fm^3, where thermal photons are produced in this model.

Table I: The strength and the anisotropy of transverse flow at each centrality.

Centrality(%)	0-10	10-20	20-30	30-40	40-50	50-60	60-70
$\langle v_r \rangle$	0.114	0.122	0.123	0.117	0.109	0.0959	0.0804
$\left\langle v_2^{\rm hydro} \right\rangle$	0.0417	0.103	0.154	0.188	0.212	0.222	0.240

From Table I, we see that the mean radial flow increases with centrality from 0-10% (b = 3.2 fm) to 20-30% (b = 7.2 fm), then decreases from 20-30% (b = 7.2 fm) to 60-70% (b = 11.7 fm). On the other hand, the mean flow anisotropy increases with centrality from 0-10% to 60-70% monotonically. One can easily understand the tendency when we investigate the time evolution of space-averaged results in Figs. 2 (a) and (b). One should notice that, for all centralities, the average radial flow is quite small before $\tau = 1$ fm/c during which most of thermal photons in $4 < p_{\rm t} < 6$ GeV/c are produced.

III. RESULTS

In Fig. 3, the v_2 of thermal photons in $0 < p_{\rm t} < 6$ GeV/c is shown for various centralities from 0 to 70% in Au+Au collisions at $\sqrt{s_{NN}} = 200$ GeV. The solid lines from bottom to top refer to centralities 0-10%, 10-20%, 20-30%, 30-40%, and 40-50%, respectively. The dashed lines from top to bottom at $p_{\rm t} = 2$ GeV/c refer to the centralities 50-60% and 60-70%.

For each centrality, the thermal v_2 increases then decreases with increasing p_t and a peak appears at $p_t \sim 2$ GeV/c. The same p_t dependence has been predicted in the study with 2+1D ideal hydrodynamics [11]. The decrease of thermal photons' v_2 at high p_t can be explained as the weak transverse flow at the early stage. Because at the higher $p_{\rm t}$, the more fraction of thermal photons are emitted from the hot matter at an early stage for all centralities. *i.e.*, at $p_{\rm t} = 3$ GeV/c, about 50% thermal photons are produced during $\tau \in (0.6, 0.9)$fm/c and at $p_{\rm t} = 4$ GeV/c, the fraction is about 70%. In our 3+1D hydrodynamics, the evolution of the radial flow is plotted in Fig. 2(a). At an early time near τ_0, *i.e.*,$\tau \in (0.6, 0.9)$fm/c, the transverse flow vanishes, and so does the elliptic flow of thermal photons. Therefore, the decrease of thermal photons' $v_2(p_t)$ at high $p_{\rm t}$ reflects the weak transverse radial flow in the early stage. Note that a similar non-trivial behavior is also seen in $p_{\rm t}$ slope parameters of dimuon spectra as a function of invariant mass [10].

Similar to the 2+1D hydrodynamics[11], small bumps appear in the elliptic flow of thermal photons at $p_{\rm t}$ close to zero. This is because of the thermal photons are emitted from two phases, QGP phase and hadronic phase at different time. In fact, thermal photon emission rate [7] is not reliable at $p_{\rm t} \to 0$.

One can also see an EOS dependence of thermal photon elliptic flow. As an example, we change from the PCE model to the FCE model, which has been employed in the conventional hydrodynamic calculations including the thermal photon calculations in the earlier study [11]. The change of the EOS is almost invisible in the $p_{\rm t}$ spectra of thermal photons due to the dominant contribution from the QGP phase. However, $v_2(p_{\rm t})$ from the hadronic phase is about ten times bigger than the one from the QGP phase. So a slight change in the hadronic phase can be magnified and become quite visible in the elliptic flow of thermal photons, as shown in Fig. 4. One can also conclude that the elliptic flow of thermal photons is sensitive to the EOS, particularly in the hadron phase. However, the effect of different EOS we obtained here is quite similar to the effect from the different formation time of quark gluon plasma [12].

The centrality dependence has been investigated in Fig.5, where (a) represents the yield and (b) the v_2 of thermal photons at midrapidity, and where different types of curves present different $p_{\rm t}$ range. It is clear that the yield of thermal photons decreases with centrality monotonously. However, the elliptic flow of thermal photons does not change with centrality monotonously. It reaches a maximum at impact parameter b=9.7fm or 40-50% centrality, then decreases for more central or more peripheral collisions, due to the interplay between the strength and the anisotropy of transverse flow. As we discussed in Sec. 2, both the strength and the anisotropy of transverse flow are important factors to generate the elliptic flow of thermal photons. The anisotropy increases with decreasing centrality, but the strength of transverse flow decreases, as shown in Table I.

In Fig.5 the $p_{\rm t}$ ranges used are (0,3)GeV/c: dotted lines; (0,6): solid lines; (0.5, 6): dashed lines; (1,6): dashed dotted lines. One can see the yield and the $p_{\rm t}$-integrate v_2 of thermal photons are not sensitive to the upper limit, c.f. the integral range (0,3) and (0,6) GeV. This is clear because the $p_{\rm t}$-spectrum of thermal photons decrease almost exponentially and high $p_{\rm t}$ region contributes very little to the total yield. The $p_{\rm t}$-spectrum of direct photons is dominant by the thermal photons at low $p_{\rm t}$region and also decreases rapidly with $p_{\rm t}$. So we can expect that the $p_{\rm t}$-integrated quantities of direct photons behaviors similarly to those of thermal photons.

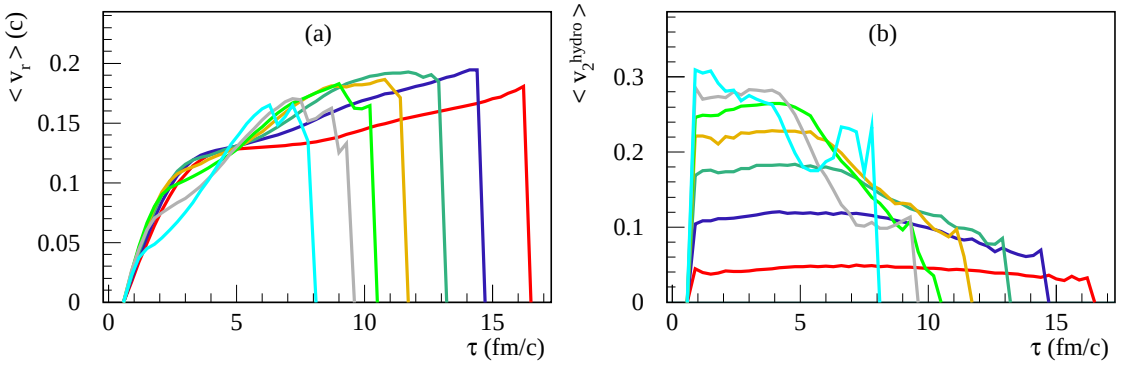

Figure 2: (Color online) Average radial flow velocity (a) and average flow anisotropy (b) as a function of proper time. Different curves correspond to 0-10%, 10-20%, ... 60-70%, respectively. A line with longer life time represents the corresponding result for a more central collision.

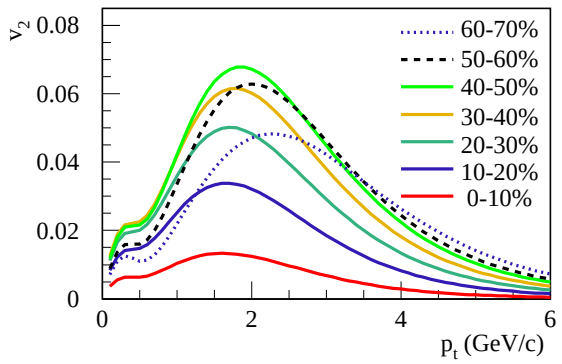

Figure 3: (Color online) v_2 for thermal photons in Au+Au collisions at $\sqrt{s_{NN}}$ = 200GeV is shown for various centralities from 0 to 70% in $0 < p_t < 6$ GeV/c. The solid lines from bottom to top correspond to centralities 0-10%, 10-20%, 20-30%, 30-40%, and 40-50%, respectively. The dashed lines from top to bottom at $p_t = 2$ GeV/c correspond to the centralities 50-60% and 60-70%.

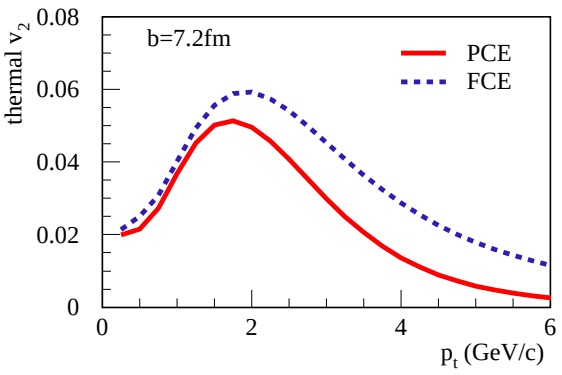

Figure 4: (Color online) The elliptic flow of thermal photons at $b = 7.2$ fm. Solid (Dashed) line is the result from a partial chemical equilibrium model (a full chemical equilibrium model).

On the other side, one can see that the yield and the p_t-integrate v_2 of thermal photons are very sensitive to the lower limit, due to the rapidly decreasing p_t-spectrum. One should be careful when a comparison between the prediction and the measurement is performed since the lower limit is experimentally determined by the detectors.

The above results are all at midrapidity. In the following we discuss the rapidity dependence, for the two scenarios: initial conditions based on EPOS flux tubes and the parameteraized one. As already said, both scenarios give many similar results. However, the rapidity dependence of elliptic flow is very different: in Fig.6, the rapidity distributions of dn/dy and the v_2 of thermal photons produced from the two kinds of initial conditions are shown. Dashed lines for parameterized one and dotted lines for EPOS. One can see thermal photon yield dn/dy has a similar dependence on rapidity y, but two very different dependences of the elliptic flow $v_2(y)$ have been obtained. One can see that $v_2(y)$ shows almost the same shape as the initial $\epsilon(\eta_s)$: A rapid decrease of elliptic flow along longitudinal direction is obtained from EPOS initial conditions, where the energy density decreases very rapidly with η_s, while a plateau of $v_2(y)$ at midrapidity region is obtained from the parameterized initial conditions. A similar observation has already been made concerning the rapidity dependence of elliptical flow of hadrons[6].

IV. DISCUSSION AND CONCLUSION

Based on a fully three-dimensional ideal hydrodynamic description of the evolution of hot and dense matter created in Au+Au collisions at $\sqrt{s_{NN}} = 200$ GeV, we found that the elliptic flow of thermal photons depends nontrivially on not only the anisotropy but also the strength of transverse flow.

At midrapidity, the v_2 of thermal photons increases with p_t up to $p_t \sim 2$ GeV/c, then decreases at higher p_t, similar to the prediction from two-dimensional ideal

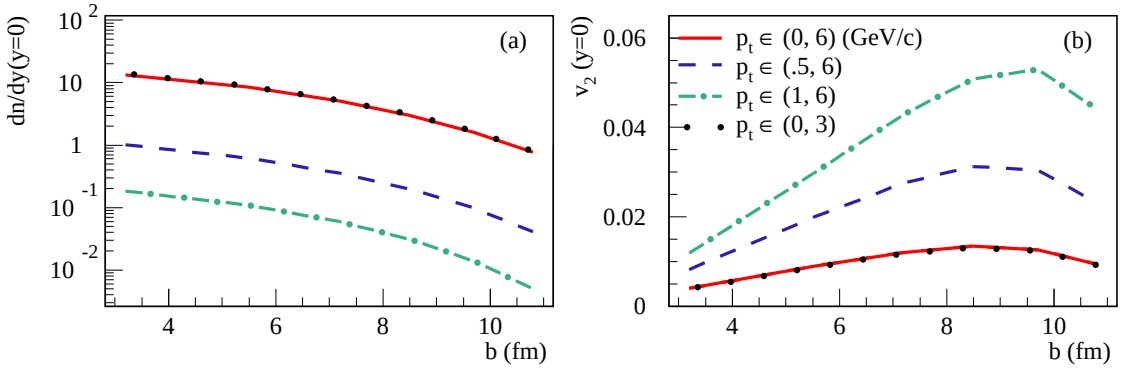

Figure 5: (Color online) (a) the yield and (b) the v_2 of thermal photons at midrapidity. Different curve types represent different p_t-integral ranges, i.e. (0,3)GeV/c: dotted lines; (0,6): solid lines; (0.5, 6): dashed lines; (1,6): dashed dotted lines.

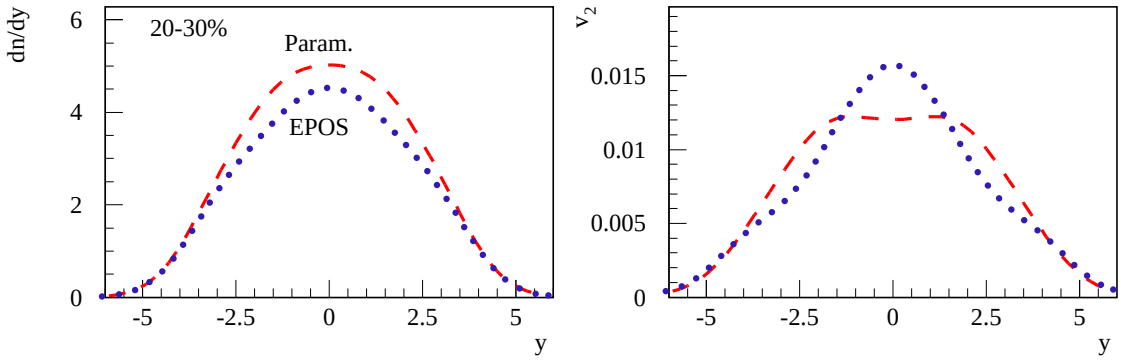

Figure 6: (Color online) (a): rapidity dependence of thermal photon production. (b): rapidity dependence of the p_t-integrate v_2 of thermal photons. Dashed lines from parameterized initial condition and dotted lines from EPOS.

hydrodynamics [11]. The decrease of thermal photon v_2 at high p_t reflects the fact that at very early times, the transverse radial flow is weak. So thermal photons can serve as a penetrating and unique probe for the whole history of the evolution.

The p_t-integrated v_2 of thermal photons increases with increasing impact parameter b up to $\sim$ 10 fm (40-50% centrality) and then decreases above. Thermal photons from two different phases have the same centrality dependence. The decrease of thermal photon v_2 at peripheral collisions is due to the interplay between the strength and anisotropy of transverse radial flow of the hot matter: As increasing impact parameter b, the anisotropy increases, but the strength of transverse radial flow decreases.

The rapidity dependence of elliptic flow of thermal photons $v_2(y)$ can "remember" the initial energy density along the longitudinal direction $\epsilon_0(\eta_s)$, *i.e.*, a plateau at midrapidity can be obtained from the parameterized initial condition based on Glauber model, while a rapid decrease of elliptic flow along rapidity is obtained from EPOS initial conditions.

Acknowledgments

This work is supported by the Natural Science Foundation of China under the project No. 10505010 and MOE of China under project No. IRT0624. The work of T.H. was partly supported by Grant-in-Aid for Scientific Research No. 19740130 and by Sumitomo Foundation No. 080734.

[1] J. W. Harris and B. Müller, Ann., Rev. Nucl. Part. Sci. **46** 71, (1996) and references therein.

[2] I. Arsene et al. [BRAHMS Collaboration], Nucl. Phys. A **757**, 1 (2005); B.B. Back *et al.*, [PHOBOS Collaboration], Nucl. Phys. A **757**, 28 (2005); J. Adams *et al.* [STAR Collaboration], Nucl. Phys. A **757**, 102 (2005); K. Adcox *et al.* [PHENIX Collaboration], Nucl. Phys. A **757**, 184 (2005).

[3] J.Y. Ollitrault, Phys. Rev. D **46**, 229 (1992); Phys. Rev. D **48**, 1132 (1993).

[4] T. Hirano, Phys. Rev. C **65**, 011901 (2002).

[5] T. Hirano and K. Tsuda, Phys. Rev. C **66**, 054905 (2002).

[6] K. Werner, T. Hirano, Iu. Karpenko, T. Pierog, S. Porteboeuf, M. Bleicher, S. Haussler, J. Phys. G: Nucl. Part. Phys. 36 (2009) 064030, arXiv:0907.5529
[7] P. Arnold, G. Moore and L.G. Yaffe, J. High Energy Phys. **0111**, 057 (2001),; J. High Energy Phys. **0112**, 9 (2001).
[8] S. Turbide, R. Rapp and C. Gale, Phys. Rev. C **69**, 014903 (2004).
[9] F. M. Liu, T. Hirano, K. Werner and Y. Zhu, Phys. Rev. C **79**, 014905 (2009) [arXiv:0807.4771 [hep-ph]].
[10] J. e. Alam, T. Hirano, J. K. Nayak and B. Sinha, arXiv:0902.0446 [nucl-th].
[11] R. Chatterjee, E. Frodermann, U. Heinz, and D.K. Srivastava, Phys. Rev. Lett. **96**, 202302 (2006).
[12] R. Chatterjee and D. K. Srivastava, arXiv:0809.0548 [nucl-th].